Available online at www.sciencedirect.com
SCIENCE DIRECT®
PERGAMON
Applied Geochemistry 18 (2003) 1095–1110
Applied Geochemistry
www.elsevier.com/locate/apgeochem

The mobility of radium-226 and trace metals in pre-oxidized subaqueous uranium mill tailings

A.J. Martin[a,*], J. Crusius[b], J. Jay McNee[a], E.K. Yanful[c]

[a]*Lorax Environmental Services, 1108 Mainland St., Vancouver, BC, Canada V6B 5L1*
[b]*University of British Columbia, Department of Earth and Ocean Sciences, Vancouver, BC, Canada V6T 1Z4*
[c]*Department of Civil and Environmental Engineering, University of Western Ontario, London, ON, Canada N6A 3K7*

Received 26 July 2002; accepted 19 November 2002
Editorial handling by R. Zielinski

Abstract

The exchange of ^{226}Ra and trace metals across the tailings-water interface and the mechanisms governing their mobility were assessed via sub-centimetre resolution profiling of dissolved constituents across the tailings–water interface in Cell 14 of the Quirke Waste Management Area at Rio Algom's Quirke Mine, near Elliot Lake, Ontario, Canada. Shallow zones (<1.5 m water depth) are characterized by sparse filamentous vegetation, well-mixed water columns and fully oxygenated bottom waters. Profiles of dissolved O_2, Fe and Mn indicate that the tailings deposits in these areas are sub-oxic below tailings depths of ~3 cm. These zones exhibit minor remobilization of Ra in the upper 5 cm of the tailings deposit; ^{226}Ra fluxes at these sites are relatively small, and contribute negligibly to the water column activity of ^{226}Ra. The shallow areas also exhibit minor remobilization of Ni, As, Mo and U. The release of these elements to the water cover is, however, limited by scavenging mechanisms in the interfacial oxic horizons. The presence of thick vegetation (*Chara* sp.) in the deeper areas (>2 m water depth) fosters stagnant bottom waters and permits the development of anoxia above the benthic boundary. These anoxic tailings are characterized by substantial remobilization of ^{226}Ra, resulting in a relatively large flux of ^{226}Ra from the tailings to the water column. The strong correlation between the porewater profiles of ^{226}Ra and Ba ($r^2 = 0.99$), as well as solubility calculations, indicate that the mobility of Ra is controlled by saturation with respect to a poorly ordered and/or impure barite phase [(Ra,Ba)SO_4]. In the anoxic zones, severe undersaturation with respect to barite is sustained by microbial SO_4 reduction. Flux calculations suggest that the increase in ^{226}Ra activity in the water cover since 1995 (from <0.5 to 2.5 Bq l^{-1}) can be attributed to an increase in the spatial distribution of anoxic bottom waters caused by increased density of benthic flora. The anoxic, vegetated areas also exhibit minor remobilization with respect to dissolved As, Ni and Zn. The removal of trace metals in the anoxic bottom waters appears to be limited by the availability of free sulphide. Collectively, the data demonstrate that while the water cover over the U mill tailings minimizes sulphide oxidation and metal mobility, anoxic conditions which have developed in deeper areas have led to increased mobility of ^{226}Ra.

1. Introduction

Scientific support for the subaqueous disposal of unoxidized, sulphide-bearing mine waste as a means of limiting acid rock drainage and metal mobility has been demonstrated for deposits in both tailings impoundments, natural lakes and coastal marine environments (Martin et al., 2001; Vigneault et al., 2001; Pedersen et al., 1993; Pedersen and Losher, 1988; MEND, 1997). The relatively-low concentrations of dissolved O_2 in water and the diffusion-limited replacement of dissolved O_2 in tailings porewater contributes to the chemical stability of sulphides in saturated environments (MEND, 1998a). Furthermore, the progressive

* Corresponding author. Fax: +1-604-688-7175.
E-mail address: ajm@lorax.bc.ca (A.J. Martin).

0883-2927/03/$ - see front matter © 2003 Elsevier Science Ltd. All rights reserved.
doi:10.1016/S0883-2927(02)00243-3

accumulation of natural sediments over time affords a diffusive barrier to sedimentary effluxes (Pedersen, 1983) and, in some cases, fosters a reducing depositional environment in which sulphides remain thermodynamically stable in perpetuity (Martin et al., 2001; Pedersen et al., 1993). At present, a dearth of data exist with respect to in situ assessments of the subaqueous stability of pyritic tailings which have been partially oxidized prior to flooding. Previous works have demonstrated that oxidized sulphides can be less stable in saturated environments than their unoxidized precursors, and that such chemical instability can be primarily attributed to the dissolution of metal sulphates and (oxy)hydroxides (Alpers et al., 1994; Ribet et al., 1995).

The flooded tailings deposits at Rio Algom's moribund operation at Quirke Mine near Elliot Lake, Ontario, provide an appropriate site to assess the efficacy of the management strategy of flooding pyritic U mill tailings that have undergone oxidation prior to submergence. Pyrite-rich tailings generated at this site were initially discharged subaerially to a series of constructed impoundments. In addition, the site provides an ideal venue to assess the factors controlling the mobility of radionuclides (e.g., Ra) from U mine tailings under a water cover. This work assesses the chemical stability of the subaqueous tailings via sub-centimetre profiling of dissolved trace metals and interstitial metabolites (e.g., dissolved O_2, H^+, SO_4^{2-}, ΣH_2S, etc.) across the tailings–water interface. Primary goals were to quantify the direction and magnitude of trace metal and Ra fluxes across the benthic boundary, and to elucidate the mechanisms controlling contaminant mobility.

2. Background and environmental setting

Field studies were conducted in Cell 14 of Rio Algom's Quirke Waste Management Area (QWMA), located ~16 km north of Elliot Lake, Ontario, Canada (Fig. 1). The Quirke Mine operated from 1956 to 1961, and again from 1968 to 1990, processing U ores using conventional leaching with H_2SO_4 and recovery via ion exchange. Prior to discharge, the tailings stream was neutralized with lime to a pH between 8.5 and 10.5. In total, ~42 million tonnes of acid-generating tailings were discharged subaerially to the QWMA. Prior to flooding in 1992, acid-generating reactions within the tailings had resulted in widespread Fe staining and the development of acidic drainage waters. Following the cessation of tailings deposition in 1990 and prior to flooding, limestone was tilled into the surface of the tailings in order to mitigate acid production (CEAA, 1996).

Cell 14 is one of a terraced arrangement of 5 cells separated by internal dykes with flow proceeding from west to east (Fig. 1). Final tailings pond decant from Cell 18 is treated to remove dissolved Ra (via coprecipitation with $BaSO_4$) prior to discharge to the receiving environment. Radium–Ba treatment sludges are deposited in cells downstream of Cell 14. Cell 14 lies at the upstream end of the series, and occupies an area of ~64 ha. At present, a water cover ranging in depth from ~0.3 m at the western margin to 3 m near the eastern dyke is actively maintained over the tailings deposits. The water column is characterized by slightly basic pH, ranging from ~7.5 to 8.5 (Rio Algom, unpublished data). Areas with water depths less than ~1.5 m are characterized by sparse filamentous vegetation and well-defined tailings–water interfaces. The density of macrophytes increases with water depth. In depths greater than 2.0 m, the cell floor hosts dense, mat-like vegetation (Muskgrass, *Chara* sp.), extending upwards from the benthic boundary to heights of up to ~40 cm. In these areas, the sediment–water interface is not visible.

3. Field and analytical methodology

Field sampling was conducted in Cell 14 of the Quirke Management Area between June 18 and July 12, 2000. The post-depositional mobility of metals in the tailings deposits and their exchange with the overlying water column was assessed by sampling of the porewaters and bottom waters using dialysis arrays (peepers). The methods for peeper preparation, deployment and subsampling are identical to those described by Martin et al. (2001), and carefully followed the protocols outlined by Carignan et al. (1994). The peepers afford 7 mm-resolution profiling of dissolved constituents (polysulphone filter, 0.45 μm pore size) from ~10 cm above the benthic boundary to a sub-interface depth of ~20 cm. Peepers were deployed at 3 sites (Q1, Q3 and Q5) for 14 days along a medial transect, hosting respective water depths of 0.43, 0.58 and 2.70 m (Fig. 1). The deployment period was long enough to ensure complete equilibration of peeper cells with adjacent porewaters. Peeper deployment was performed via insertion by a diver, and the placement of the peeper photographed to determine precisely (±2 mm) the peeper position at the tailings–water interface.

Sub-millimetre profiling (200 μm vertical increments) of dissolved O_2 was conducted across the tailings–water interface on diver-collected cores (butyrate core tubes, 8 cm i.d.). collected at 3 sites (Q1, Q3 and Q6) using custom-made O_2 microelectrodes identical to those used by Archer et al. (1989). Due to the dense benthic flora present at Station Q5, a sediment core could not be obtained at this site. Quadruplicate profiles were collected from each core, except Q6 where duplicate profiles were taken. During profiling, cores were kept in the

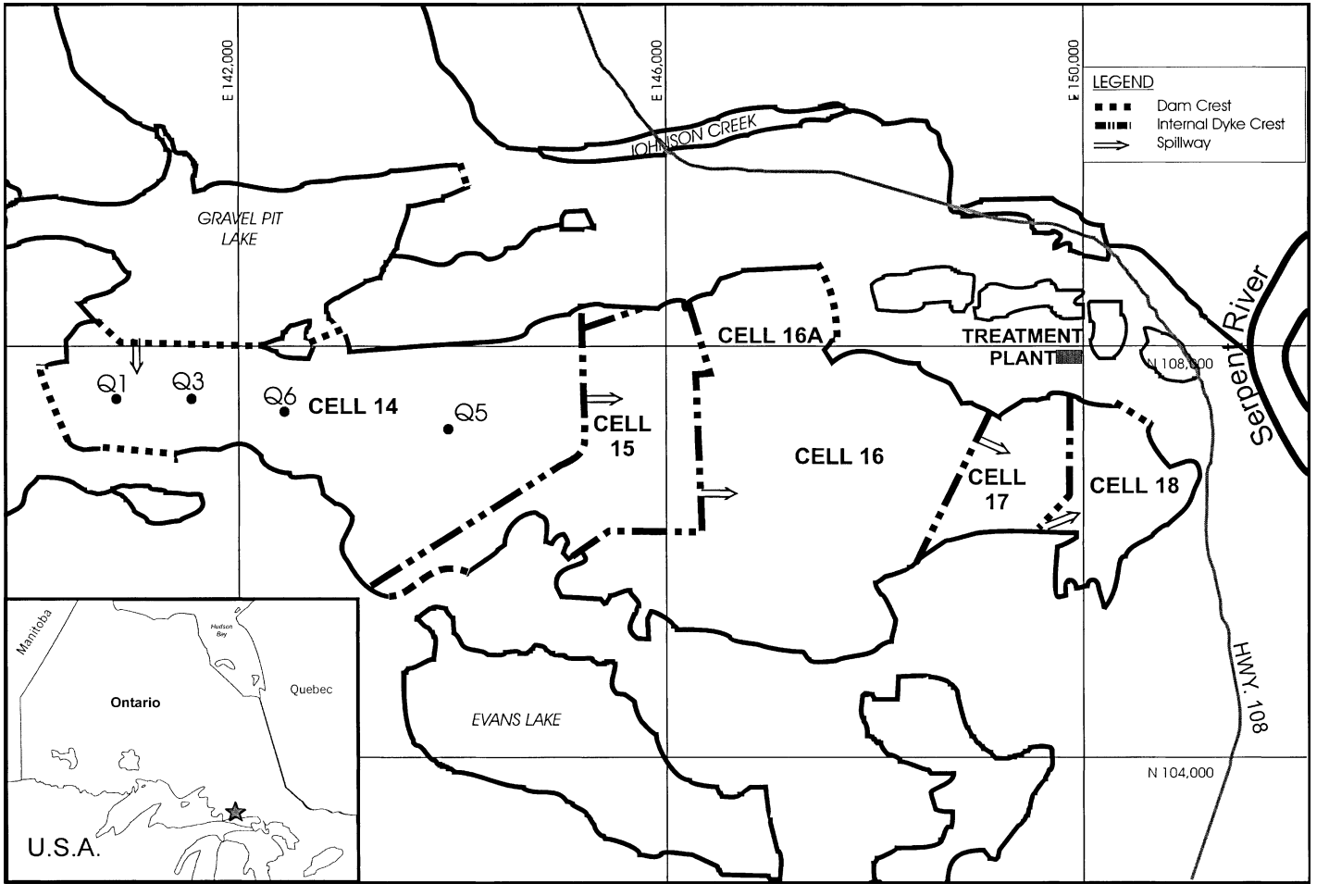

Fig. 1. Sampling locations in Cell 14 of the Quirke Waste Management Area.

shade to minimize photosynthetic activity by benthic algae in the surficial sediments (Jørgensen et al., 1979).

For solid-phase analysis of sediments, additional cores were retrieved at 3 sites (Q1, Q3 and Q6) via diver collection using butyrate core tubes (8 cm i.d.). Cores were extruded in 1 cm intervals. All sediment subsamples were frozen until analysis for total metals, carbonate-C and total C, N and S.

Peeper samples (6 ml from each peeper compartment) were analyzed for a suite of dissolved metals (Mn, Fe, Ni, Cu, Zn, As, Mo, Ba, Pb, ^{226}Ra and U) and interstitial metabolites (NO_3^-, SO_4^{2-}, ΣH_2S, pH and alkalinity). Determinations of metal concentrations were performed by ICP-MS (Mn, Ni, Cu, Zn, As, Mo, Cd, Ba, Pb and U) and GFAAS (Fe) as described by Martin et al. (2001). Samples were analyzed for ^{226}Ra following the methods described by Godoy (1990). Nitrate and SO_4^{2-} were analyzed by ion chromatography (Fishman and Friedman, 1985), while ΣH_2S measurements were determined using the spectrophotometric method of Cline (1969). Measurements of porewater pH were conducted in peeper cells by direct puncturing of the filter membrane using a combination needle pH microelectrode.

Sediment samples for solid phase analysis were freeze-dried and ground to 200 mesh in a tungsten-carbide mill. Concentrations of major and minor elements were determined by X-ray fluorescence spectrometry using tetraborate glass beads and pressed powders for major and minor elements, respectively, as described in Calvert (1990). A range of international geochemical reference standards (Abbey, 1983) was used for instrument calibration. Total C and S concentrations were determined by combustion/gas chromatography as described by Pedersen et al. (1993). Carbonate–C was determined by coulometry. Organic C was determined from the difference between the total and carbonate-C values.

4. Results and discussion

4.1. Sediment geochemistry

Solid-phase concentrations of Ni, Cu and Zn in both oxidized and unoxidized zones are within the background ranges observed for crustal rocks (Table 1) and are similar to values reported for these tailings elsewhere (e.g., Peacey et al., 2002). Uranium, As and Pb, however, are enriched in the tailings over crustal concentrations by roughly an order of magnitude. The tailings host variable organic-C content, with values ranging up to 0.5 wt.% near the tailings–water interface.

The tailings deposits in Cell 14 are dominated by quartz (65–95 wt.%), muscovite (1.3–10%), K-feldspar (1.4–11 wt.%) and pyrite (1–8%) (Peacey et al., 2002). Limestone applications have resulted in variable calcite concentrations ranging from 3.5 to 17%. The tailings are also characterized by abundant gypsum (4.2–18%) (Peacey et al., 2002), likely originating from both the neutralization of the acidic mill stream as well as from in situ precipitation associated with extensive pyrite oxidation during the pre-flood period. The tailings are potentially acid generating; the net neutralization potential has been measured to be −61.4 kg $CaCO_3$ eq./t (Paktunc and Dave, 2000). The tailings deposits also contain approximately 30,000 tonnes of sewage sludge from the municipal water treatment plant which were co-deposited with the tailings.

There is unequivocal evidence to suggest that the tailings deposits in the QWMA had undergone oxidation prior to flooding. First, aerial photographs indicate widespread Fe staining on the tailings surface prior to limestone additions and flooding in 1992. Furthermore, water quality measurements conducted on surface seepages prior to flooding were characterized by low pH values (~pH 3; Rio Algom, unpublished data). In addition, visual inspection of the tailings cores at stations Q1, Q3 and Q6 demonstrated the presence of stained, oxidized material to depths ranging from 2 to 3 cm. In these cores, partially oxidized orange-brown tailings graded sharply into gray, unoxidized tailings below. XRD analysis indicates that pyrite in the upper oxidized horizons has been depleted to <1 wt.% (Peacey et al., 2002). The presence of oxidized tailings phases has also been verified via mineralogical analysis which has identified secondary goethite (Paktunc and Dave, 2000).

4.2. Dissolved oxygen micro-profiles

Dissolved O_2 (DO) profiles at Q1 and Q6 are very similar (Fig. 2). Convex-upward profiles below 1 mm depth in the porewaters are indicative of diffusion and consumption of DO within the tailings. DO at these sites is completely removed from pore solution in the top 3 mm of the tailings deposit. DO profiles measured across the tailings–water interface at Q3 are characterized by porewater O_2 maxima at depths ranging from 1 to 3 mm below the benthic boundary (Fig. 2). Max-

Table 1
Solid-phase metal concentrations in tailings in Cell 14 in comparison to average crustal abundances from Weast (1985)

Element	QWMA tailings[a] (mg/kg)	Crustal abundance (mg/kg)
U	25±13	2.7
Ni	24±11	75
Cu	48±8	55
Zn	24±11	70
Pb	157±20	12.5
As	31±4	1.8

[a] Mean±1 standard deviation ($n=18$).

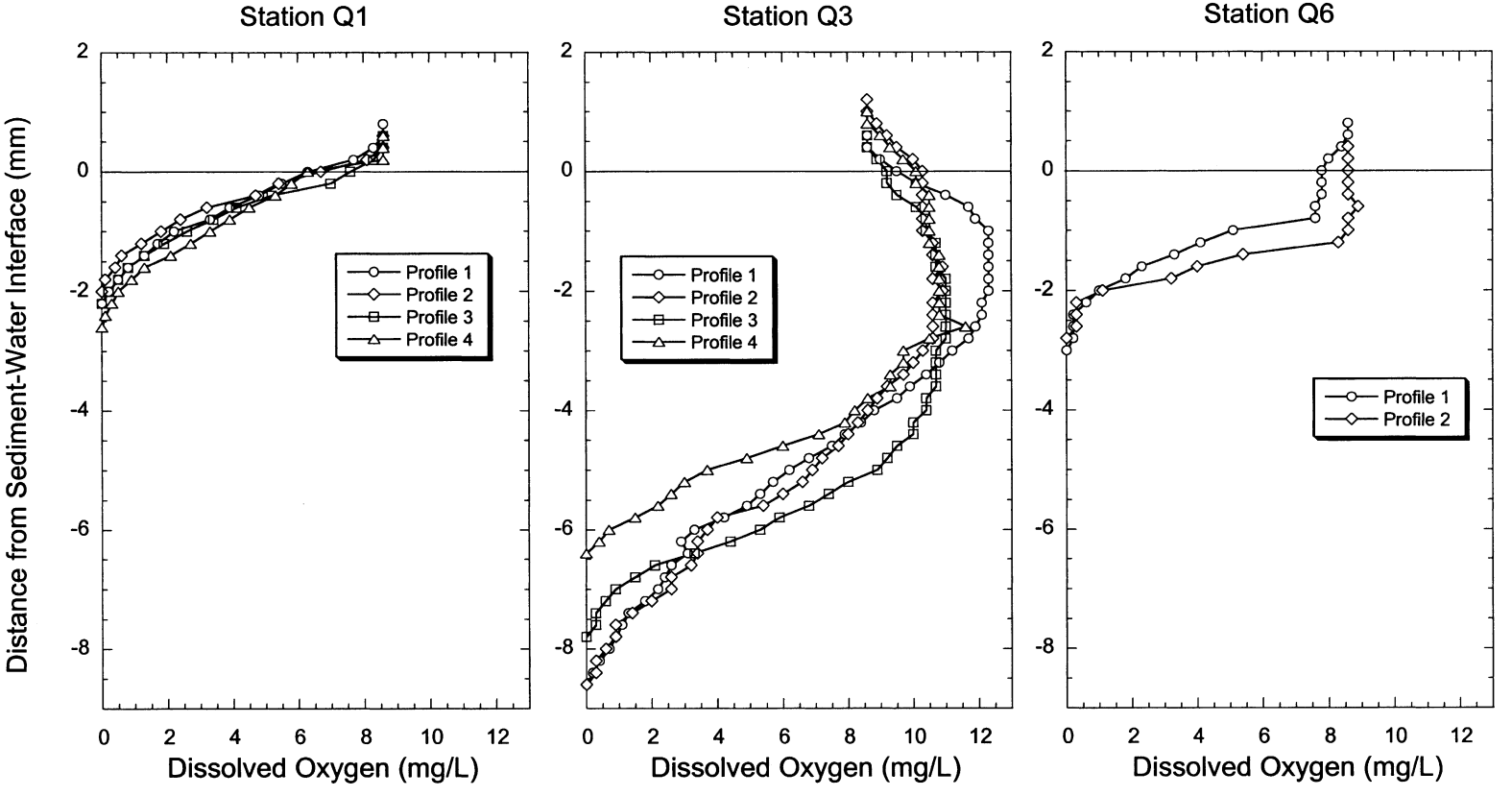

Fig. 2. Dissolved O_2 micro-profiles across the tailings–water interface at stations Q1, Q3 and Q6.

imum DO concentrations of ~12 mg/l at tailings depths ranging from 1 to 2 mm reflect supersaturation caused by O_2 production in the near-surface horizons. The DO maxima at Q3 can be attributed to the production of O_2 by photosynthetic benthic algae in the interfacial horizons. Previous studies have also demonstrated increases in DO concentrations due to photosynthesis in shallow (1–4 mm) porewaters of tailings (Vigneault et al., 2001), sediments (Revsbech and Jørgensen, 1986) and algal mats (Revsbech and Ward, 1983). The consumption of DO below the zone of O_2 production results in near-linear decreases in DO to undetectable levels at depths ranging from ~6.5 to 8.5 mm (Fig. 2).

The consumption of DO within the surficial tailings deposits can likely be attributed to the oxidation of labile organic matter (OM) and/or the oxidation of residual sulphides (e.g., pyrite). Profiles of % organic-C at Q1 and Q3 demonstrate that OM has accumulated in the uppermost 1–2 cm of the tailings deposit (Fig. 3). Irrespective of the O_2 consumption pathway, the shallow penetration depth of DO implies that the potential for sulphide oxidation is limited to the uppermost 1 cm of the tailings deposit. Such observations are consistent with other field measurements of DO penetration in submerged tailings (Vigneault et al., 2001; Elberling and Damgaard, 2001).

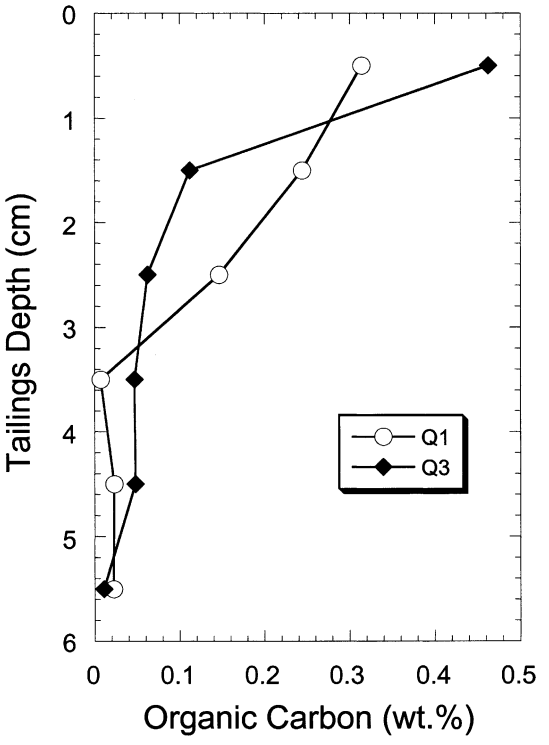

Fig. 3. Depth distributions of organic-C concentration in submerged tailings at Stations Q1 and Q3, in Cell 14 of the Quirke Waste Management Area.

4.3. Metal mobility in shallow, unvegetated areas

The profiles of dissolved Fe and Mn at the shallow, sparsely vegetated sites (Q1 and Q3) exhibit considerable similarity (Figs. 4 and 5). The uniform concentrations of these constituents above the tailings–water interface are indicative of a well-mixed water column. Concomitant increases in the porewater concentrations of dissolved Mn and Fe occur in the upper 5 cm of the sediment column at Q1 and Q3 and reflect the reductive dissolution of Fe- and Mn-bearing (oxy)hydroxides (Froelich et al., 1979). The depletion of Fe below the porewater maximum at Q1 reflects the removal of Fe(II) from pore solution (Fig. 4). Such removal likely reflects the precipitation of authigenic carbonate (e.g., siderite) and/or Fe-sulphide phases (e.g., FeS; Suess, 1979).

At Q1 and Q3, SO_4 concentrations increase with depth below the tailings–water interface to maxima of 370 and 1200 mg/l, respectively (Figs. 4 and 5). The absence of dissolved O_2 below 1 cm (Fig. 2) suggests that the observed SO_4 profiles cannot be attributed to acid-generating reactions occurring at depth within the tailings. Moreover, the abundance of dissolved Fe (presumable as Fe^{2+}) at depths of 3 cm at measured circumneutral pH precludes the existence of O_2 below this depth (Stumm and Morgan, 1981). Sulphate in the tailings porewaters most likely originates from the dissolution of gypsum which originated from both the neutralization of the acidic tailings slurry in the mill prior to discharge, as well as from secondary gypsum which has formed in situ. The linearity of the SO_4 concentration gradients at Q1 and Q3 suggests that the source of SO_4 is deeper than the peeper penetration depth (i.e., greater than 10 cm) (Figs. 4 and 5). Such a tenet is supported by XRD analysis which indicates that gypsum primarily occurs below tailings depths of >5 cm in the deposits (Peacey et al., 2002). The gypsum distribution most likely represents a pre-flooding signature associated with extensive pyrite oxidation in the vadose zone and resulting export of SO_4^{2-} and precipitation of gypsum at deeper tailings depths (Blowes and Jambor, 1990).

The trace metal profiles at Q1 and Q3 are similar, and demonstrate that the shallow zones are characterized by minor remobilization of As, Mo, U and Ni (Figs. 4 and 5). The As data closely mirror the associated profiles of dissolved Fe, in which both elements are characterized by remobilization at depth, upward diffusion, and re-precipitation in the near-surface oxic horizons. Such behaviour suggests As concentrations may be controlled by sorption with Fe (oxy)hydroxides, and is consistent with As cycling observed in other mining-impacted systems (Azcue et al., 1994; McCreadie et al., 2000; Martin and Pedersen, 2002). The similarity between the Mo and Mn profiles, particularly at Station Q3, suggests Mo is remobilized in concert with the dissolution of Mn

(oxy)hydroxides (Figs. 4 and 5). Such observations are consistent with Mo–Mn associations in marine systems (Shimmield and Price, 1986). Dissolved U profiles at Stations Q1 and Q3 are characterized by progressively increasing concentrations with depth, and likely reflect the upward diffusion of U from a source deeper than the peeper penetration depth (>7 cm) (Figs. 4 and 5). The abundance of HCO_3^- (20–60 mg/L) in the porewaters at these sites suggests that the mobility of U is governed by the formation of stable U(VI)–carbonate complexes (Abdelouas et al., 1998).

Nickel concentrations increase in the porewaters in a similar manner to Fe, and suggest a component of the solid-phase Ni inventory may be associated with Fe (oxy)hydroxides (Figs. 4 and 5). Nickel–Fe associations have been shown to be important in oxidized mine tailings (Ribet et al., 1995) and freshwater sediments (Tessier et al., 1996). Alternatively, the general linearity of the Ni profiles may indicate that the source of Ni is deeper than the peeper penetration depth (>7 cm). The strong correlation between Ni and SO_4^{2-} supports this tenet, and may imply that the source of

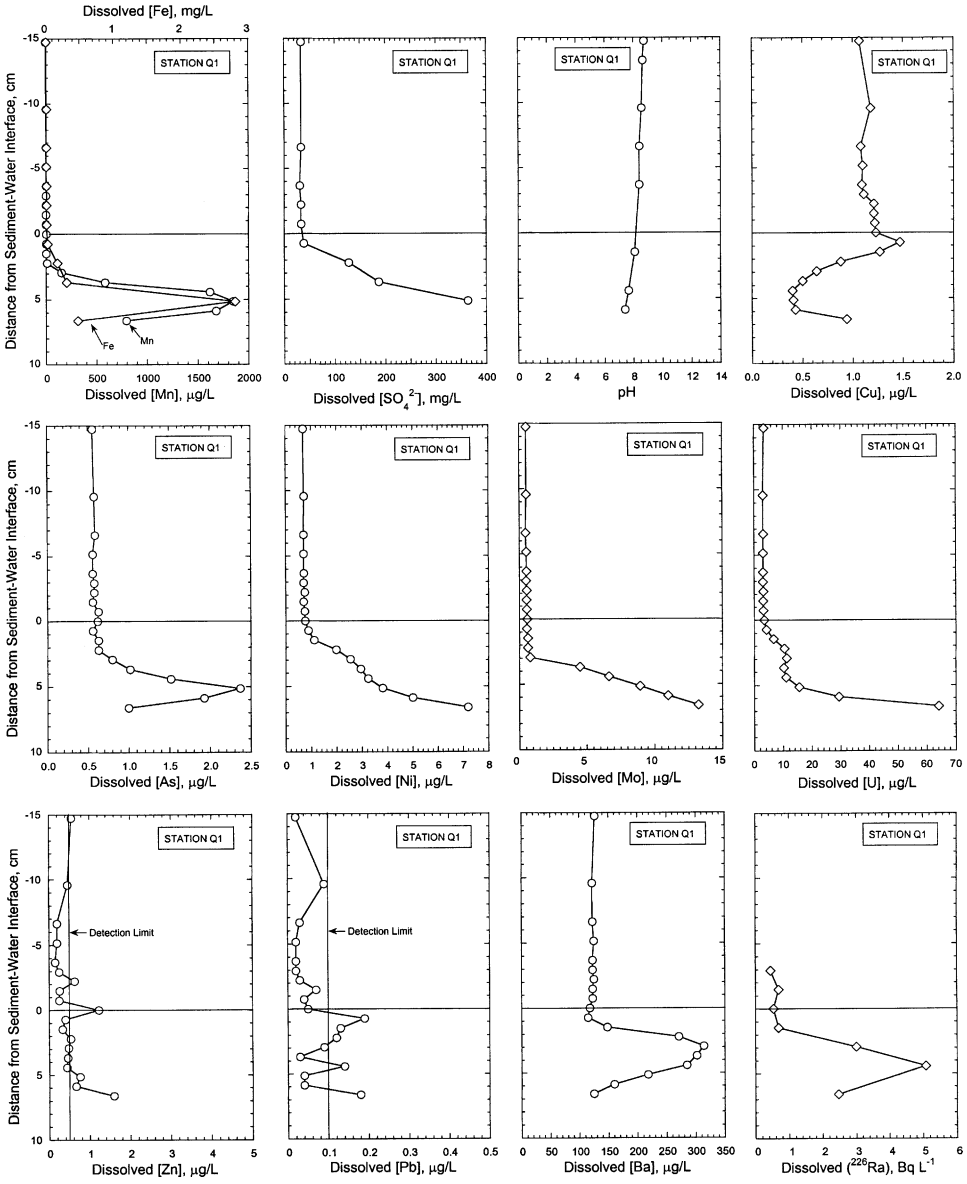

Fig. 4. Depth distributions of dissolved (<0.45 µm) Mn, Fe, SO_4^{2-}, pH, Mo, U, As, Ni, Cu, Zn, Pb, Ba and ^{226}Ra across the tailings–water interface at Station Q1.

labile Ni represents a secondary phase which precipitated at depth in the vadose zone during the preflood period in response to the export of oxidation products from the surface tailings and reprecipitation at depth. The minor remobilization of Ni within these deposits is consistent with the results from laboratory lysimeter tests using U mill tailings from Quirke Mine which showed Ni release from the submerged tailings (MEND, 1998b).

The decrease in dissolved Cu concentrations below the tailings–water interface at Q1 and Q3 reflects the removal of Cu from pore solution, and indicates that the tailings deposits are serving as a sink for dissolved Cu below a depth of 1 cm (Figs. 4 and 5). The precipitation of a Cu-sulphide phase (e.g., Huerta-Diaz et al., 1998) presents the most likely rationale to account for the Cu removal at these sites. Although ΣH_2S was undetectable (<32 μg l^{-1}) in the tailings porewaters, its presence cannot be discounted. Indeed, CuS is very insoluble ($-\log K = 36.1$; Stumm and Morgan, 1981) and may readily precipitate at exceedingly-low free sulphide concentrations (i.e., at values <32 μg l^{-1}). Zinc

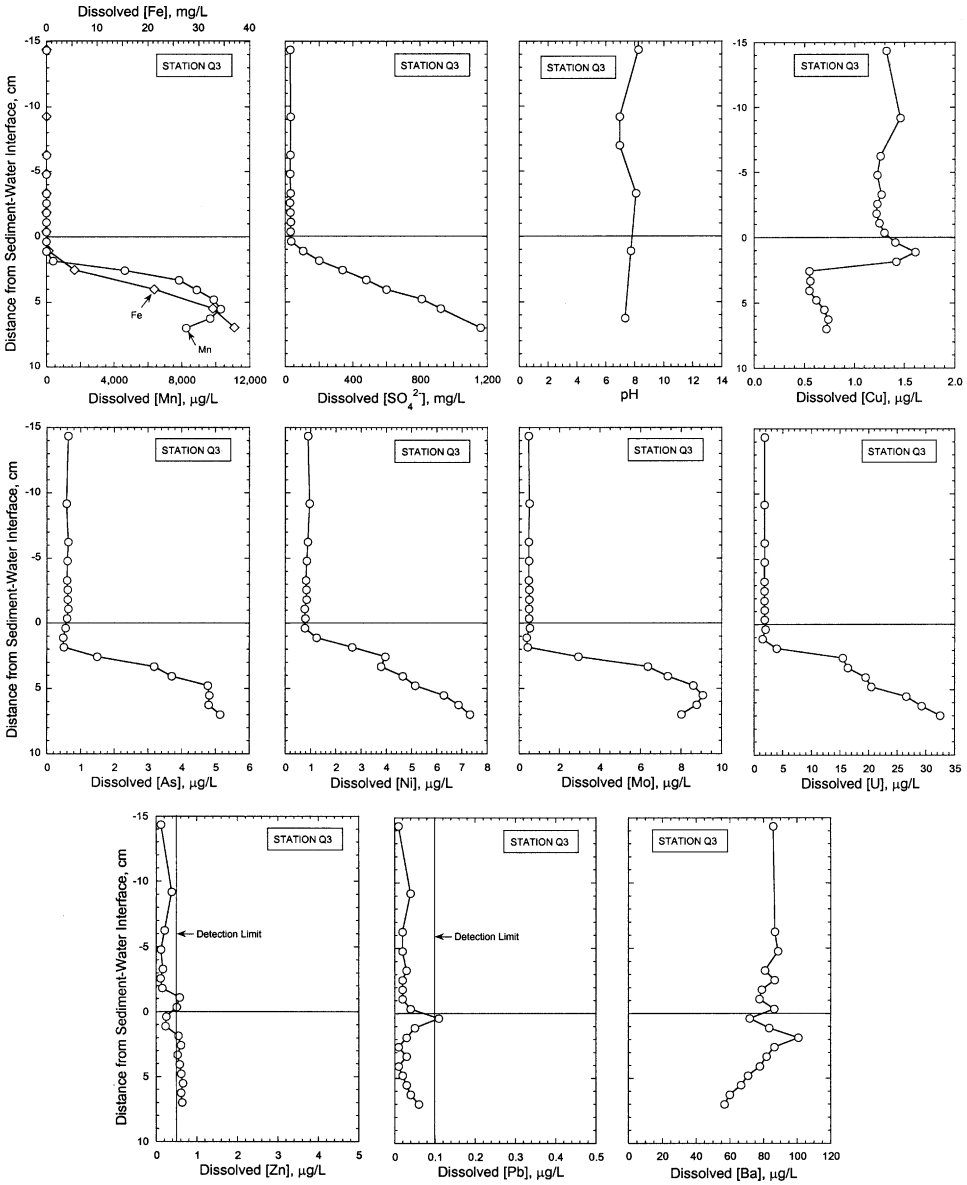

Fig. 5. Depth distributions of dissolved (<0.45 μm) Mn, Fe, SO_4^{2-}, pH, Mo, U, As, Ni, Cu, Zn, Pb and Ba across the tailings–water interface at Station Q3.

and Pb are not significantly remobilized within the tailings; concentrations at Q1 and Q3 were near or below their respective detection limits of 0.5 μg/l and 0.1 μg/l, respectively, throughout all sampled horizons (Figs. 4 and 5).

Although Fe is intensely remobilized in sub-oxic depths within the unvegetated tailings, the commensurate remobilization of associated trace elements is exceedingly low. Such observations imply that the labile Fe(III) phases do not host significant concentrations of trace elements.

4.4. Metal mobility in deep, vegetated areas

Deeper regions of the tailings pond (>2 m water depth) are considerably more reducing than the shallow areas. The data suggest the deep waters are both anoxic and sulphidic, as indicated by elevated levels of dissolved Mn, Fe and ΣH_2S in the bottom waters at site Q5 (Fig. 6). The Fe and Mn profiles indicate that Fe(II) and Mn(II) are remobilized from the tailings solids via the reductive dissolution of (oxy)hydroxide phases (Fig. 6). The decrease in ΣH_2S values with depth likely

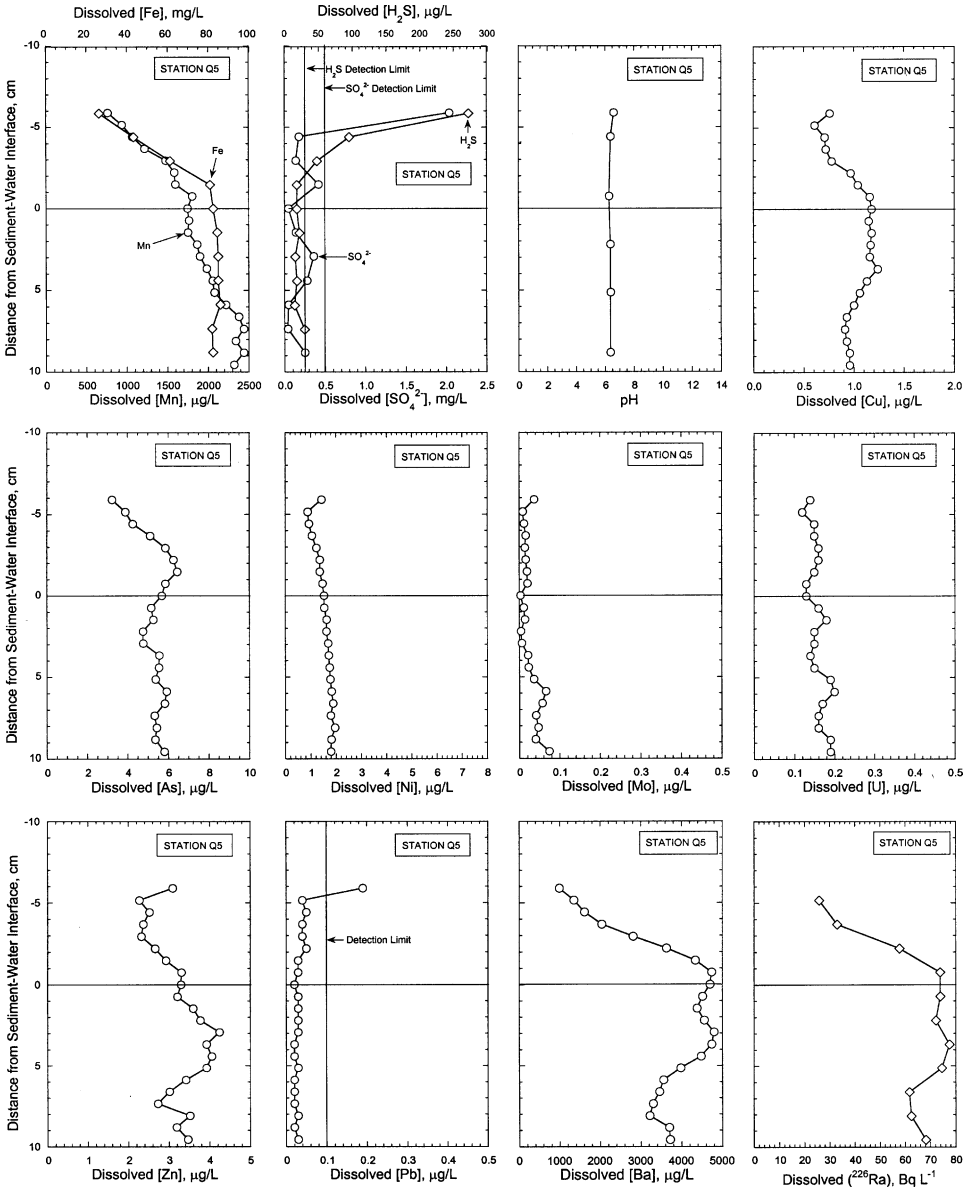

Fig. 6. Depth distributions of dissolved (<0.45 μm) Mn, Fe, SO_4^{2-}, ΣH_2S, pH, Mo, U, As, Ni, Cu, Zn, Pb, Ba and ^{226}Ra across the tailings–water interface at Station Q5.

reflects the precipitation of Fe-sulphide phases in the bottom waters.

Steep gradients in Mn, Fe and ΣH_2S attest to substantial stratification in the deep water column. The presence of thick vegetation (*Chara* sp.) in the deeper areas fosters stagnant bottom waters and permits the development of stratification above the benthic boundary. Specifically, the dense flora, which extends above the tailings–water interface to heights of 30–40 cm, acts as a physical barrier which restricts mixing. Solute transport in these zones is likely dominated by eddy diffusion. The absence of DO near the benthic boundary implies that the rate of DO consumption (e.g., via bacterial respiration of organic matter) exceeds the rate of supply associated with the exchange of oxygenated surface waters and photosynthetic reactions.

The contrasting redox conditions at Q5 have a pronounced effect on metal mobility. Bottom water concentrations of As, Ni and Zn at Q5 are slightly elevated above the water column concentrations observed at Q1 and Q3, indicating that the reducing conditions prevalent at Q5 result in increased mobility of these elements (Fig. 6). As proposed for Q1 and Q3, the mobility of As at Q5 is likely governed by the redox cycling of Fe. The data suggest that Ni and Zn are remobilized concomitantly with Fe(II) and/or via the dissolution of soluble metal-bearing SO_4 phases. The relatively high concentrations of As, Ni and Zn in the reducing bottom waters (~1.5 and 3.5 μg/l, respectively) suggest that their removal via sulphide precipitation is limited by the availability of free sulphide. Dissolved Cu is characterized by uniformly low concentrations (~0.6–1.2 μg/l) throughout all sampled horizons, and Pb concentrations at Q5 were undetectable (<0.1 μg/l), below a bottom water depth of 5 cm (Fig. 6). In summary, the generally low and invariant values for dissolved Ni, Cu, Zn and Pb across the tailings–water interface implies that the anoxic conditions in the deeper vegetated areas of the pond severely limit the mobility of these elements.

In contrast with the shallow sites, dissolved U and Mo concentrations remain low and invariant across the tailings–water interface. Low dissolved U values probably reflect the reduction of U(VI) to U(IV) which is then removed from solution via precipitation of highly insoluble U(IV) (Langmuir, 1978). Low concentrations of dissolved Mo likely reflect removal via sulphide precipitation. Mo has been shown to associate with Fe-monosulphides (Bertine, 1972), authigenic pyrite (Huerta Diaz and Morse, 1992) and discrete Mo-sulphides (Bertine, 1972).

4.5. Factors governing the mobility of ^{226}Ra and Ba

The activity of ^{226}Ra in surface waters of Cell 14 has exhibited a sinusoidal increase since 1995, with annual maxima increasing from 0.3 to ~2.5 Bq/l between 1995 and 2001 (Fig. 7). Annual maximum and minimum values are typically observed in the late fall and spring, respectively. The cyclicity can be in part related to seasonal freeze–thaw cycles. Samples are collected from surface waters at the discharge spillway to Cell 15 (Fig. 1), and accordingly, exhibit low ^{226}Ra activity during periods of active snowmelt in the spring due to dilution. Surface inflows to Cell 14 consist solely of inputs from Gravel Pit Lake, which lies upstream of mining-related influences. Run-off from the surrounding

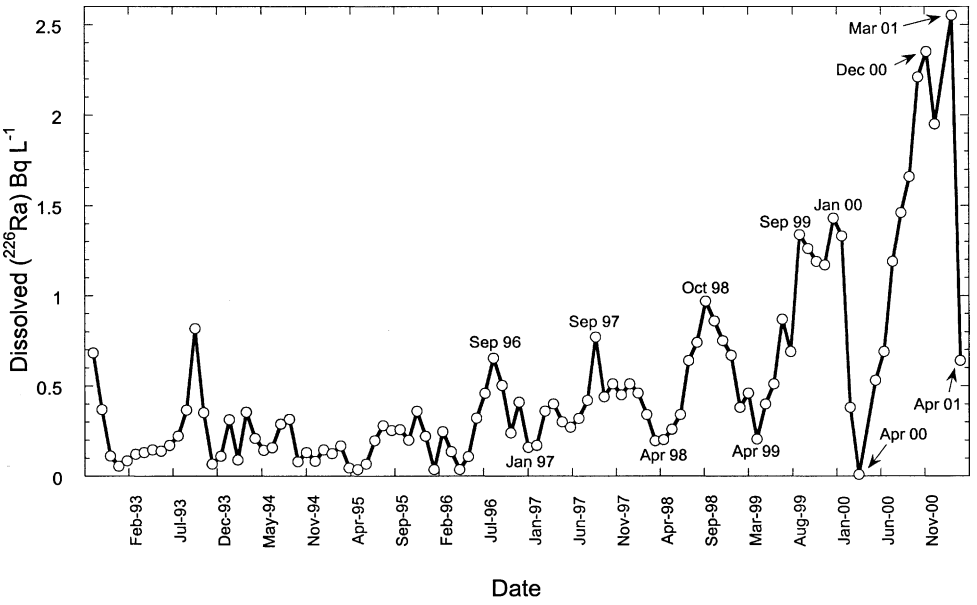

Fig. 7. Activity of ^{226}Ra in surface waters at the decant of Cell 14 between 1993 and 2001 (Rio Algan, unpublished data).

berms is insignificant. Accordingly, the available evidence suggests the inventory of ^{226}Ra in surface waters of Cell 14 is derived from sources within the tailings impoundment.

In order to elucidate the controls governing the mobility of Ra, comparisons were made to the distributions of Ba. Radium acts as a chemical analog of Ba, and as a result, the two elements tend to cycle together in aquatic environments (Paige et al, 1998; Moore, 1997; Carroll et al., 1993). Concordant behaviour of Ra and Ba in U mill tailings (Snodgrass and Hileman, 1985) is also the basis for Ra removal from U-mill waste streams via coprecipitation with $BaSO_4$ (barite). Porewater data demonstrate that Ba and Ra are remobilized concomitantly within the tailings deposits in Cell 14 (Figs. 4 and 6). However, the invariant values for both Ba and ^{226}Ra across the tailings–water interface at Q1 indicate that the shallow unvegetated tailings in Cell 14 do not contribute significantly to the water column inventories of these elements (Fig. 4). The magnitude of Ra and Ba remobilization is considerably greater in the anoxic deposits at Q5; ^{226}Ra activity increases in bottom waters to values exceeding 70 Bq l^{-1} (Fig. 6).

The porewater data suggest that the remobilization of Ra within the tailings is governed by the dissolution of a Ba-containing SO_4 phase. Regression analysis of the Ba and Ra distributions for both Q1 and Q5 illustrates the strong relationship between the two elements (Fig. 8). Possible phases include Ra and Ba associated with gypsum and/or Ra associated with a Ra-bearing barite phase [$(Ra,Ba)SO_4$]. Both gypsum and barite have been identified via XRD and SEM analyses (Peacey et al., 2002). Gypsum dissolution has been invoked to account for Ra mobility in laboratory assessments of submerged U mill tailings (MEND, 1998b). However, examination of barite solubility within the tailings deposits (see below) suggests that barite dissolution is the principal source of Ra in Cell 14. A previous study of U mill tailings in the Elliot Lake area also concluded that Ra is preferentially associated with $BaSO_4$ and sparingly associated with gypsum (Snodgrass and Hileman, 1985).

Porewater Ba and SO_4^{2-} data were used to calculate saturation indices (SI) for barite using PHREEQC (Parkhurst and Appelo, 2000). SI values at the shallow sites (Q1 and Q3) increase from a value of ~0.3–0.5 in the water column to a maximum value of ~1.3–1.5 at a tailings depth of ~5 cm, suggesting that both the water column and tailings are supersaturated with respect to pure barite (Fig. 9). However, the shapes of the SI profiles, and in particular, the uniform SI values in the porewaters below depths of 5 cm suggest that true saturation with respect to the Ba-hosting phase differs from that predicted for pure, crystalline barite (Fig. 9). The data indicate "apparent" saturation between an SI

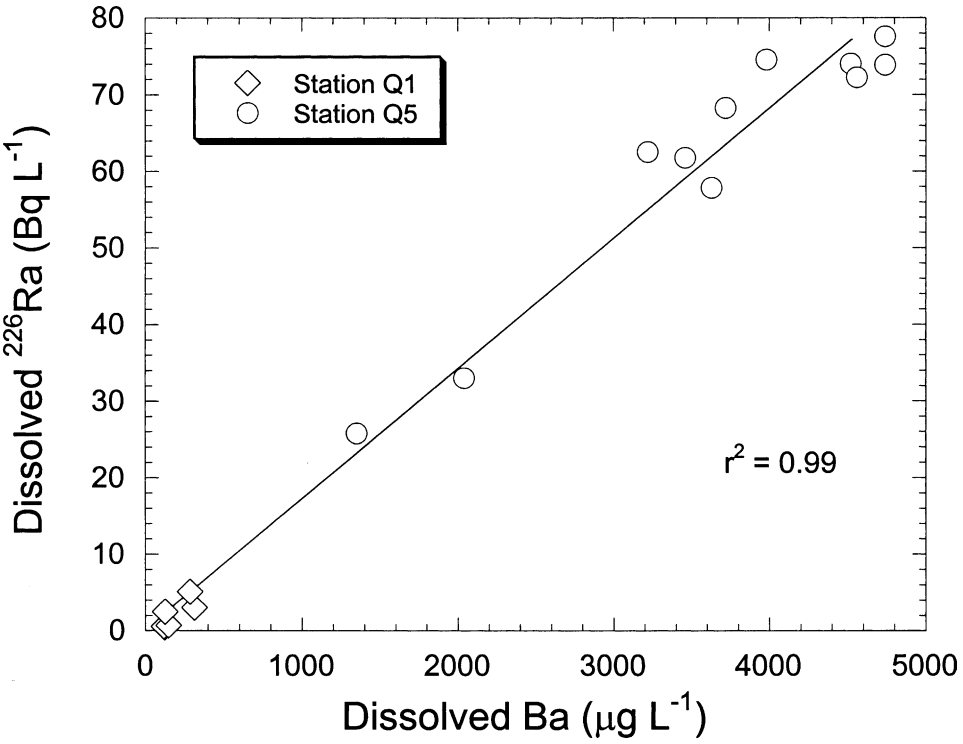

Fig. 8. Scatter plot of dissolved (<0.45 µm) ^{226}Ra activity vs. Ba concentration in the bottom waters and tailings porewaters at Stations Q1 and Q5.

range of 1.3 and 1.6. If the apparent saturation index is adopted, it can be assumed that the water column and surficial sediments (uppermost 4–5 cm) at Q1 and Q3 are undersaturated with respect to the Ba phase. The discrepancy between the predicted (SI = 0) and apparent (SI = 1.3–1.6) saturation index is explained if the barite present in the surficial sediments is amorphous, or the barite contains substantial amounts of impurities such as Sr. Either of these possibilities could lead to Ba and SO_4^{2-} concentrations that exceed the values expected for saturation with pure, crystalline barite (McManus et al., 1998; Rushdi et al., 2000).

The SI profiles at the deep site (Q5) contrast greatly with those from the shallow areas (Fig. 9). Precise SI values could only be determined for the uppermost sample at Q5, as all those horizons below exhibited SO_4^{2-} concentrations below the detection limit (~0.5 mg/l) (Fig. 6). In order to provide a possible upper limit of SI values, Ba and SO_4^{2-} solubility products were calculated using the SO_4^{2-} detection limit of 0.5 mg/l. From this limiting calculation, the SI values at Q5 are lower than those at Q1 and Q3 by at least an order of magnitude. The porewaters at Q5, therefore, are characterized by severe barite undersaturation throughout all sampled horizons.

The inter-station variability with respect to the degree of barite saturation can be related to the redox contrasts between the shallow unvegetated zones and the deep vegetated areas. Specifically, the large magnitude of barite undersaturation at Q5 is due to strong SO_4 reduction which maintains undetectable levels of SO_4 in the pond bottom waters and tailings porewaters. In these stagnant, anoxic zones, SO_4 represents the terminal electron acceptor used in the microbially-mediated oxidation of organic matter. This in situ evidence for the microbial-driven release of Ra is consistent with laboratory studies which have demonstrated that the release of Ra associated with both U mill tailings (Landa et al., 1986) and (Ba, Ra)SO_4 treatment sludges (Fedorak et al., 1986) is greatly enhanced in the presence of SO_4-reducing bacteria. Conversely, the diffusion of unreduced SO_4 towards the tailings–water interface at Q1 and Q3 maintains saturation with respect to barite below tailings depths of 5 cm. Hence, the magnitude of porewater Ba and Ra activities, and the associated fluxes of these elements from the tailings to the pond water column, are limited by saturation with respect to barite. Given the above considerations, it is proposed that the observed increases in Ra activity in surface waters of Cell 14 since 1995 can be related to the progressive expansion and intensity of reducing conditions at the sediment-water interface, which in turn can be related to the gradual increase in the spatial extent and density of benthic flora.

The absence of benthic flora (and hence anoxic bottom waters) in the shallow areas of the pond can likely be attributed to ice contact with the tailings during the winter months. A survey of the pond conducted in March 2001 revealed ice in direct contact with the tailings west of Station Q6 (Lorax, unpublished data). The inhibition of macrophyte recolonization in these areas acts to maintain oxygenated bottom waters during the ice-free period, thereby enhancing the chemical stability of barite (and hence ^{226}Ra).

4.6. Fluxes across the tailings–water interface

Porewater data were used to calculate metal fluxes across the tailings–water interface using Fick's First Law (Table 2):

$$J_z = \frac{-D_j^0}{F}\phi\frac{\mathrm{d}c}{\mathrm{d}z}$$

where J_z is the flux; D_j^o = diffusion coefficient (Li and Gregory, 1974); F = formation factor of 2 for silty sand (Ullman and Aller, 1982); ϕ = porosity of 0.7 (Peacey et al., 2002); and $\mathrm{d}c/\mathrm{d}z$ = the concentration gradient across the tailings–water interface. The diffusive flux calculations do not take into account transport mechanisms such as bioturbation and irrigation, which can increase the net diffusive flux by a factor of 2–6 (Rivera-Duarte and Flegal, 1994). In addition, physical processes such as wave-induced transport and gas ebullition have been ignored. Therefore, the diffusive effluxes in Table 2 may provide conservatively low estimates of the total benthic flux. Fluxes at Station Q5 were calculated by using the gradients in the bottom waters. In reality, eddy diffusion in addition to molecular diffusion will drive transport through the vegetated zone. Therefore, both ϕ and F were assigned a value of 1. Accordingly, the flux estimates for Q5 are predicted to be conservatively low.

Flux estimates from each site were used to assess the contributions of the porewater fluxes to water column concentrations by assuming steady-state, a mean water depth of 1.5 m, and a water residence time of 135 days (Rio Algom, unpublished data). Given these assumptions, the fluxes of Ni, Cu, Zn, As, Mo and U contribute negligibly to the water column concentrations of these metals in Cell 14 (Table 2). This result suggests that water cover concentrations of these metals are largely influenced by surface inflows and meteoric waters. The minor contributions from submerged tailings undoubtedly reflect the combined effects of the small degree of remobilization within the tailings, and the scavenging of many metals by Fe and Mn oxy(hydroxides) in oxic surficial horizons or as sulphides in anoxic horizons. The implication, therefore, is that the submerged tailings deposits are chemically stable with respect to remobilization of Ni, Cu, Zn, As, Mo and U to surface waters (Table 2).

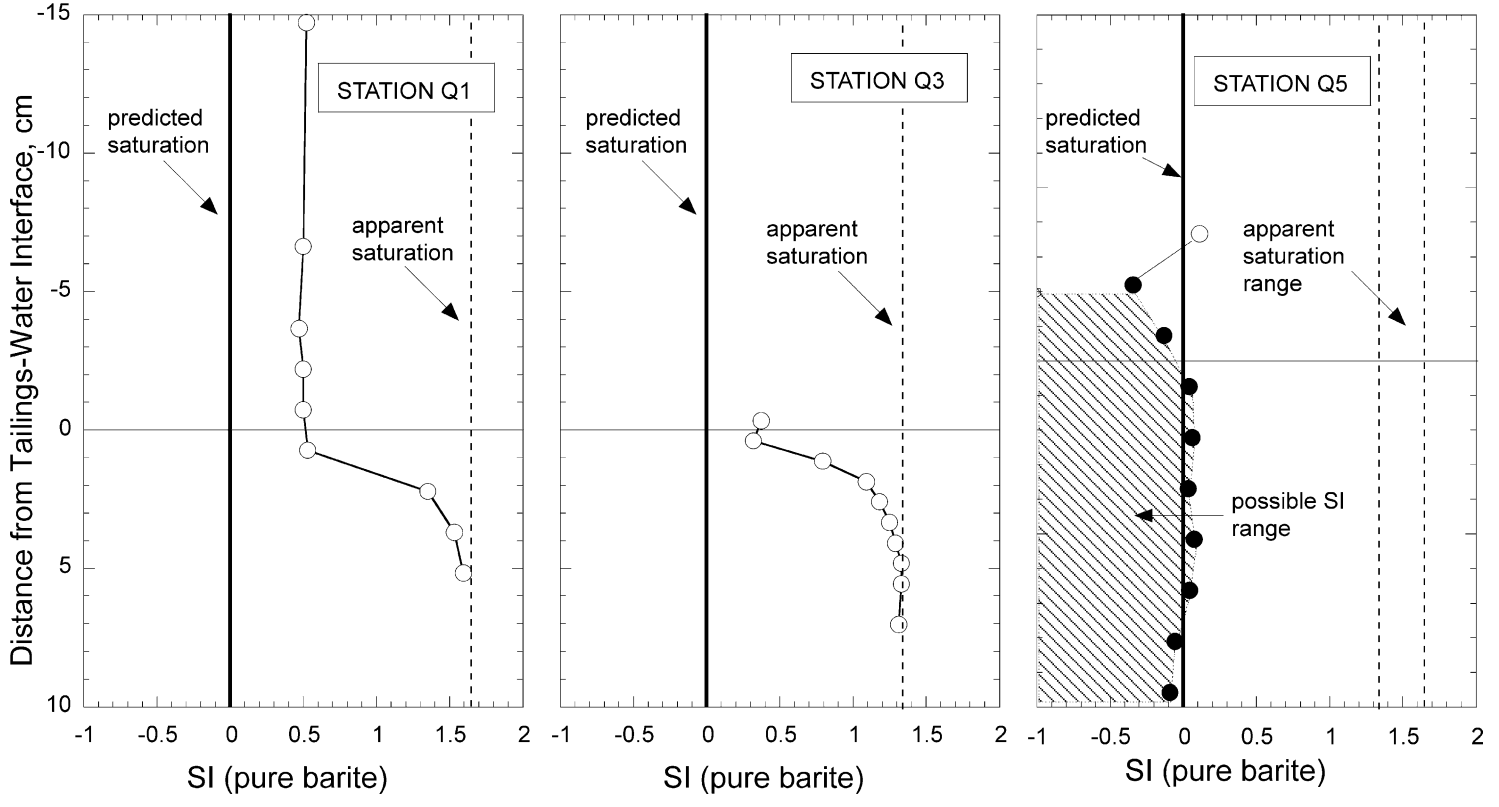

Fig. 9. Depth distributions of saturation indices with respect to pure barite ($BaSO_4$) at Stations Q1, Q3 and Q5, including SI values based on measured Ba and SO_4^{2-} concentrations (○) and SI values based on measured Ba concentrations and a SO_4^{2-} detection limit value of 0.5 mg/L (●). Predicted saturation and apparent saturation points are indicated.

Similar calculations for ^{226}Ra demonstrate that tailings overlain by anoxic bottom waters (i.e., vegetated areas) represent the principle source of ^{226}Ra activity in surface waters of Cell 14. Assuming the calculated Ra flux applies to one half of the pond area (i.e., estimated extent of vegetated zone), diffusive transport of ^{226}Ra to the water column could support an activity of 5.2 Bq l^{-1}. This value is comparable to the maximum ^{226}Ra activity of ~2.5 Bq l^{-1} measured in March 2001 (Fig. 7).

4.7. Implications for tailings management

With regards to the long-term management of the tailings deposits in Cell 14, attention should be focussed

Table 2
Diffusive flux estimates and associated water column impacts for dissolved Ni, Cu, Zn, As, Mo, U and ^{226}Ra in Cell 14 of the Quirke Management Area

Station	Element	Dj[a] (cm^2 s^{-1})	dc/dz[b] (g cm^{-4})	Flux[c] (J_z) (μg cm^{-2} y^{-1})	Predicted steady-state water column concentration[d] (μg l^{-1})	Observed water column concentration[e] (μg l^{-1})
Q1	Ni	6.23E-06	−9.46E-11	0.01	0.02	ND
Q3	Ni	6.23E-06	−4.19E-11	0.03	0.07	0.8
Q5	Ni	6.23E-06	−1.76E-10	0.01	0.03	0.7
Q1	Cu	6.50E-06	−3.24E-10	0.02	0.06	ND
Q3	Cu	6.50E-06	−1.49E-10	0.01	0.03	1.3
Q5	Cu	6.50E-06	2.70E-10	−0.02	−0.05	1.1
Q1	Zn	6.57E-06	NC	NC	NC	ND
Q3	Zn	6.57E-06	NC	NC	NC	<0.5
Q5	Zn	6.57E-06	2.03E-10	−0.02	−0.04	<0.5
Q1	As	8.20E-06	−1.35E-11	0.001	0.003	ND
Q3	As	8.20E-06	5.41E-11	−0.005	−0.012	0.6
Q5	As	8.20E-06	−6.76E-10	−0.061	−0.15	0.6
Q1	Mo	8.94E-06	−6.76E-12	0.001	0.002	ND
Q3	Mo	8.94E-06	−5.41E-11	0.005	0.010	0.5
Q5	Mo	8.94E-06	−4.05E-12	0.001	0.001	0.5
Q1	U	3.91E-06	−9.46E-10	0.04	0.10	ND
Q3	U	3.91E-06	−1.89E-10	0.01	0.02	1.8
Q5	U	3.91E-06	−5.41E-11	0.002	0.006	2.0
Station	Element	Dj[a] (cm^2 s^{-1})	dBq/dz[b] (Bq cm^{-4})	Flux[c] (J_z) (Bq cm^{-2} y^{-1})	Predicted steady-state water column activity[d] (Bq l^{-1})	Observed water column activity (Bq l^{-1})
Q1	^{226}Ra	7.86E-06	−1.02E-10	0.009	0.02	ND
Q5	^{226}Ra	7.86E-06	−1.70E-08	3.01	10.4	2.5

ND: Not determined; NC: not calculable due to detection limit considerations.

[a] D_j^o = in situ diffusion coefficient at 20 °C.

[b] dc/dz = the concentration gradient across the tailings-water interface.

[c] Positive fluxes represent transport from the tailings to the overlying water column.

[d] Steady-state water column concentration represents impact to water column based on porewater fluxes. Impact estimates assume flux applies to entire pond area of Cell 14, a steady-state water depth of 1.5 m and an estimated flushing time of 135 days. Positive values represent metal addition to water column; negative values represent removal from water column.

[e] Observed water column value in surface waters at the time of sampling. Surface water samples not collected at Q1

on minimizing Ra mobility via vegetation control measures. One possible means of achieving this would be to lower water levels in the pond as much as possible prior to freeze-up in order to take advantage of ice-scouring mechanisms. This will have a continuing benefit by preventing vegetation from establishing in the shallow zones, thus minimizing the potential for anoxia to develop during the ice-free periods. Furthermore, the addition of nutrients and/or organic matter to the pond system as a means to maximize sulphide mineral stability is not recommended. First, the present degree of metal immobility does not warrant organic matter amendments. Second, such actions could promote increased sediment O_2 demand, potentially leading to the onset of SO_4 reduction in the shallow areas of the pond. The development of anoxia near the tailings-water interface in the shallow zones of Cell 14 could in turn lead to further undersaturation and destabilization of the Ba–Ra host phase.

5. Conclusions

The porewater data suggest that the subaqueous storage of the potentially acid-generating U mill tailings in Cell 14 is an effective means to minimize acid generation and mobility of Ni, Cu, Zn, As, Mo, Pb and U. The shallow unvegetated areas exhibit minor remobilization of Ni, As, Mo and U in the suboxic porewaters; however, release of these elements to the water cover is limited by scavenging mechanisms in the interfacial oxic horizons. Conversely, the subaqueous environments in the deep areas of Cell 14, which maintain permanent anoxia owing to the presence of dense benthic vegetation, favour the mobilization of Ra and Ba and the release of these elements to surface waters. Given the role of benthic macrophytes in creating anoxic conditions that enhance Ra release, and given the fact the vegetation was absent prior to flooding, the data strongly suggest that the increase in spatial distribution and density of benthic flora has contributed to the observed increase in ^{226}Ra activity since tailings submergence. Remediation measures for minimizing ^{226}Ra mobility should be focussed on controlling the growth and distribution of benthic macrophytes.

Acknowledgements

Funding for this study was provided by Rio Algom Ltd, and was made possible through a collaborative research program with the University of Western Ontario (UWO). Thanks go to Art Coggan and Roger Payne of Rio Algom for their interest and support. The logistical efforts of Jody Stefanich (Elliot Lake Research Field Station) and field support of Vicky Peacy (UWO) were also greatly appreciated. We also thank Bill Burnett of Florida State University for conducting the ^{226}Ra analysis.

References

Abbey, S., 1983. Studies in standard sample of silicate rocks and minerals, 1969–1982. Geol. Surv. Canada.

Abdelouas, A., Lutze, W., Nuttall, E., 1998. Chemical reactions of uranium in groundwater at a mill tailings site. J. Contam. Hydrol. 34, 343–361.

Alpers, C.N., Blowes, D.W., Nordstrom, D.K., Jambor, J.L., 1994. Secondary minerals and their relative solubility. In: Jambor, J.L., Blowes, D.W. (Eds.), Environmental Geochemistry of Sulfide Mine-Wastes. Mineralogical Association of Canada. Waterloo, Ontario, Canada, pp. 247–270.

Archer, D., Emerson, S., Smith, C.R., 1989. Direct measurement of the diffusive sublayer at the deep sea floor using oxygen microelectrodes. Nature 340, 623–626.

Azcue, J.M., Mudroch, A., Rosa, F., Hall, G.E.M., 1994. Effects of abandoned gold mine tailings on the arsenic concentrations in water and sediments of Jack of Clubs Lake, B.C. Environ. Tech. 15, 669–678.

Bertine, K.K., 1972. The deposition of molybdenum in anoxic waters. Mar. Chem. 1, 43–53.

Blowes, D.W., Jambor, J.L., 1990. The pore-water geochemistry and the mineralogy of the vadose zone of sulfide tailings, Waite Amulet, Quebec, Canada. Appl. Geochem. 5, 327–346.

Calvert, S.E., 1990. Geochemistry and origin of the Holocene sapropel in the Black Sea. In: Ittekkot, V., Kempe, S., Michaelis, W., Spitzy, A. (Eds.), Facets of Modern Biogeochemistry. Springer-Verlag, pp. 326–352.

Carignan, R., St-Pierre, S., Gächter, R., 1994. Use of diffusion samplers in oligotrophic lake sediments: effects of free oxygen in sampler material. Limnol. Oceanog. 39, 468–474.

Carroll, J., Falkner, K.K., Brown, E.T., Moore, W.S., 1993. The role of the Ganges-Brahmaputra mixing zone in supplying barium and ^{226}Ra to the Bay of Bengal. Geochim. Cosmochim. Acta 57, 2981–2990.

CEAA, 1996. Decommissioning of Uranium Mine Tailings Management Areas in the Elliot Lake Area. Canadian Environmental Assessment Agency, June 1996.

Cline, J.D., 1969. Spectrophotometric determination of hydrogen sulphide in natural waters. Limnol. Oceanog. 14, 454–458.

Elberling, B., Damgaard, L.R., 2001. Microscale measurements of oxygen diffusion and consumption in subaqueous sulfide tailings. Geochim. Cosmochim. Acta 65, 1897–1905.

Fishman, M.J., Friedman L.C., 1985. Methods for Determination of inorganic Substances in Water and Fluvial Sediment. US Geol. Surv. Rep.

Fedorak, P.M., Westlake, D.W.S., Anders, C., Kratochvil, B., Motkosky, N., Anderson, W.B., Huck, P.M., 1986. Microbial release of Ra-226 from (Ba,Ra)SO_4 sludges from uranium mine wastes. Appl. Environ. Microbiol. 52, 262–268.

Froelich, P.N., Klinkhammer, G.P., Bender, M.L., Luedtke, N.A., Heath, G.R., Cullen, D., Dauphin, P., Hammond, D., Hartman, B., 1979. Early oxidation of organic matter in

pelagic sediments of the eastern equatorial Atlantic: suboxic diagenesis. Geochim. et Cosmochim. Acta 43, 1075–1090.

Godoy, J.M., 1990. Methods for measuring radium isotopes: gross alpha and gross beta counting. In: The Environmental Behaviour of Radium. Technical Report Series, 310. Vol. 1. International Atomic Energy Agency.

Huerta-Diaz, M., Morse, J.W., 1992. Pyritization of trace metals in anoxic marine sediments. Geochim. Cosmochim. Acta 56, 2681–2702.

Huerta-Diaz, M.A., Tessier, A., Carignan, R., 1998. Geochemistry of trace metals associated with reduced sulphur in freshwater sediments. Appl. Geochem. 13, 213–233.

Jørgensen, B.B., Revsbech, N.P., Blackburn, T.H., Cohen, Y., 1979. Diurnal cycle of oxygen and sulfide microgradients and microbial photosynthesis in a cyanobacterial mat sediment. Appl. Environ. Microbiol. 38, 46–58.

Landa, E.R., Miller, C.L., Updegraff, D.M., 1986. Leaching of Ra-226 from U mill tailings by sulfate-reducing bacteria. Health Phys. 51, 509–518.

Langmuir, D., 1978. Uranium solution-mineral equilibria at low temperatures with applications to sedimentary ore deposits. Geochim. Cosmochim. Acta 42, 547–569.

Li, Y.H., Gregory, S., 1974. Diffusion of ions in sea water and in deep-sea sediments. Geochmim. Cosmochim. Acta 38, 703–714.

Martin, A.J., McNee, J.J., Pedersen, T.F., 2001. The reactivity of sediments impacted by metal-mining in Lago Junin, Peru. J. Geochem. Explor. 74, 179–191.

Martin, A.J., Pedersen, T.F., 2002. Seasonal and inter-annual mobility of arsenic in a lake impacted by metal mining. Env. Sci. Technol. 36, 1516–1523.

McCreadie, H., Blowes, D.W., Ptacek, C., Jambor, J.L., 2000. Influence of reduction reactions and solid-phase composition on porewater concentrations of arsenic. Env. Sci. Technol. 34, 3159–3166.

McManus, J., Berelson, W.M., Klinkhammer, G.P., Johnson, K.S., Coale, K.H., Anderson, R.F., Kumar, N., Burdige, D., Hammond, D.E., Brumsack, H.J., McCorkle, D.C., Rushdi, A., 1998. Geochemistry of barium in marine sediments: implications for its use as a paleoproxy. Geochim. Cosmochim. Acta 62, 3453–3473.

MEND, 1997. Review of Water Cover Sites and Research Projects. Mine Environment Neutral Drainage Program, Natural Resources Canada, Report 2.18.1.

MEND, 1998a. Design Guide for the Subaqueous Disposal of Reactive Tailings in constructed Impoundments. Mine Environment Neutral Drainage Program, Natural Resources Canada, Report 2.11.9.

MEND, 1998b. Wet Barriers on Pyritic Uranium Tailings. Part III. Laboratory Diffusion Lysimeter Studies of Uranium Tailings Deposited under a Shallow Water Cover. Mine Environment Neutral Drainage Program, Natural Resources Canada, Report 2.13.1b.

Moore, W.S., 1997. High fluxes of radium and barium from the mouth of the Ganges-Brahmaputra River during low river discharge suggest a large groundwater source. Earth Planet. Sci. Lett. 150, 141–150.

Paige, C.R., Kornicker, W.A., Hileman, O.E., Snodgrass, W.J., 1998. Solution equilibria for uranium ore processing: the $BaSO_4$-H_2SO_4-H_2O system and the $RaSO_4$-H_2SO_4-H_2O system. Geochim. Cosmochim. Acta 62, 15–23.

Paktunc, A.D., Dave, N.K., 2000. Prediction of acidic drainage and accompanying metal releases from unsegregated pyritic uranium mill tailings based on effluent chemistry and post leaching sample mineralogy. In: Internat. Conf. Acid Rock Drainage, Denver, CO, pp. 891–900.

Parkhurst, D.L., Appelo, C.A.J., 2000. User's Guide to PHREEQC (Version 2)—A Computer Program for Spection, Batch-Reaction, One-Dimensional Transport, and Inverse Geochemical Calculations. United States Geological Survey.

Peacey, V., Yanful, E.K., Payne, R., 2002. Field study of geochemistry and solute fluxes in flooded uranium mine tailings. Can. Geotech. J. 39, 357–376.

Pedersen, T.F., 1983. Dissolved heavy metals in a lacustrine mine tailings deposit-Buttle Lake, British Columbia. Mar. Poll. Bull. 14, 249–254.

Pedersen, T.F., Losher, A.J., 1988. Diagenetic processes in aquatic mine tailings deposits in British Columbia. In: Forstner, W. (Ed.), Chemistry and Biology of Solid Waste. Springer-Verlag, Berlin, pp. 238–258.

Pedersen, T.F., Mueller, B., McNee, J.J., 1993. The early diagenesis of submerged sulphide-rich mine tailings in Anderson Lake, Manitoba. Can. J. Earth Sci. 30, 1099–1109.

Revsbech, N.P., Jørgensen, B.B., 1986. Microelectrodes: their use in microbial ecology, Adv. Microb. Ecol. 9, pp. 293–352.

Revsbech, N.P., Ward, D.M., 1983. Oxygen microelectrode that is insensitive to medium chemical composition: use in an acid microbial mat dominated by *Cyanobacterium caldarium*. Appl. Environ. Microbiol. 45, 755–759.

Ribet, I., Ptacek, C., Blowes, D.W., Jambor, J.L., 1995. The potential for metal release by reductive dissolution of weathered mine tailings. J. Contam. Hydrol. 17, 239–273.

Rivera-Duarte, I., Flegal, A.R., 1994. Benthic lead fluxes in San Francisco Bay, California, USA. Geochim. Cosmochim. Acta 58, 3307–3313.

Rushdi, A.I., McManus, J., Collier, R.W., 2000. Marine barite and celestite saturation in seawater. Mar. Chem. 69, 19–31.

Shimmield, G.B., Price, N.B., 1986. The behaviour of molybdenum and manganese during early sediment diagenesis-offshore Baja California, Mexico. Mar. Chem. 19, 261–280.

Snodgrass, W.J. and Hileman, O.E., 1985. On the Geochemical Mechanism Controlling Ra-226 Dissolution in Uranium Mill Wastes (Tailings). Uranium Tailings Program, Energy Mines and Resources, Government of Canada.

Stumm, W., Morgan, J.J., 1981. Aquatic Chemistry. Wiley-Interscience, New York.

Suess, E., 1979. Mineral phases formed in anoxic sediments by microbial decomposition of organic matter. Geochim. Cosmochim. Acta 43, 339–352.

Tessier, A., Fortin, D., Belzile, N., DeVitre, R.R., Leppard, G.G., 1996. Metal sorption to diagenetic iron and manganese oxyhydroxides and associated organic matter: narrowing the gap between field and laboratory measurements. Geochem. Cosmochim. Acta 60, 387–404.

Ullman, W.J., Aller, R.C., 1982. Diffusion coefficients in nearshore sediments. Limnol. Oceanog. 27, 552–556.

Vigneault, B., Campbell, P., Tessier, A., DeVitre, R., 2001. Geochemical changes in sulfidic mine tailings stored under a shallow water cover. Water. Res. 35, 1066–1076.

Weast, R.C., 1985. CRC Handbook of Chemistry and Physics, sixty-sixth ed. CRC Press, Boca Raton, FL.